CFC2.pdf

Single-Scattering Optical Tomography

Vadim A. Markel and John C. Schotland
Departments of Radiology and Bioengineering, University of Pennsylvania, Philadelphia, PA 19104
215-746-3014; vmarkel@mail.med.upenn.edu

Abstract: We propose a novel tomographic method which utilizes visible or near-infrared light as a probe in the "mesoscopic" scattering regime when the tissue exhibits sufficiently strong scattering, yet the detected light is not diffuse.

OCIS codes: (170.0170) Medical optics and biotechnology; (170.6960) Tomography

Traditional tomographic imaging relies on probing tissue with particles or waves which experience almost no scattering inside the human body. Consequently, scattering has historically been viewed as an obstruction to imaging. Approximately fifteen years ago, a novel tomographic technique was suggested which makes use of strongly scattered (diffuse) near-infrared (NIR) light [1,2]. While NIR radiation can easily penetrate many centimeters into most types of human tissue, it experiences scattering on the characteristic scale of 1 mm. Diffuse NIR tomography has numerous potential advantages. However, the associated inverse problem is nonlinear and ill-posed. This has, so far, limited the clinical utility of diffuse optical methods.

Both the limit of geometrical propagation without scattering (typical of x-rays in computerized tomography) and the limit of strong scattering (typical of NIR light in diffuse optical tomography) have been extensively explored. However, the intermediate scattering regime has received much less attention. By the intermediate or "mesoscopic" scattering regime we mean here the situation when scattering is significant enough so that noncollinear measurements can be performed, yet the characteristic sample size is no larger than a few scattering lengths. Neither geometrical optics nor the diffusion equation can be used to describe the propagation of light in this regime. Instead, the radiative transport equation (RTE) must be used. If only a few scattering events are important the RTE can be readily solved by the collision expansion. If one retains in this expansion only the first correction to ballistic (geometrical) propagation, a very efficient and accurate tomographic technique can be obtained. We will refer to this technique as the single scattering optical tomography (SSOT).

The physical principle of SSOT is quite simple. Consider a sample in the shape of a slab. A narrow collimated ray of light enters in the normal direction through one of the slab's surfaces. In the absence of scattering, the ray would propagate straight through the slab. Detection of such straight (unscattered) rays is the basis of computerized x-ray tomography. If there is finite scattering in the medium, the ray can "change direction". In SSOT, only the intensity of such broken rays is detected by means of angularly-selective detectors which are non-collinear with the source. It can be shown that the intensity measured by the detector is mathematically related to the integral of the attenuation coefficient taken along the single-scattered ray.

The potential advantages of SSOT include linearity and well posedness of the inverse problem (in contrast to the optical diffusion tomography). Further, SSOT does not require phase measurements (in contrast to the optical coherence tomography (OCT)) and can be performed using a single projection or in backscattering (in contrast to the x-ray tomography). It utilizes non-ionizing radiation and can exploit additional contrast mechanisms compared to OCT and x-ray tomography. Finally, the inverse problem of the SSOT is two-dimensional and image reconstruction can be performed slice-by-slice.

We have performed simulation of SSOT image reconstruction in a rectangular scattering sample with dimensions $L_x \times L_y \times L_z$. The forward data were obtained by solving the RTE numerically. We have used the isotropic scattering function. In this case, the RTE can be reduced to a three-dimensional integral equation [3,4]. The equation was solved by discretization of the volume of the sample with the step h. The sample dimensions were $L_x = 11h$, $L_y = 122h$ and $L_z = 40h$. The background absorption coefficient of the sample was $\mu_a = 0.01h^{-1}$ which was spatially modulated by absorbing inhomogeneities (the target) as is explained below. The scattering coefficient was constant throughout the sample, $\mu_s = 0.08h^{-1}$. The sources were normally incident on the surface $z = 0$. The detectors were placed on the other side of the sample and measured the specific intensity exiting the surface $z = L_z$ at the angle of $\pi/4$ with respect to the z-axis. Reconstruction of the total attenuation coefficient $\mu_t = \mu_a + \mu_s$ was performed in slices $x = x_{\rm slice} = {\rm const}$ separated by the

CFC2.pdf

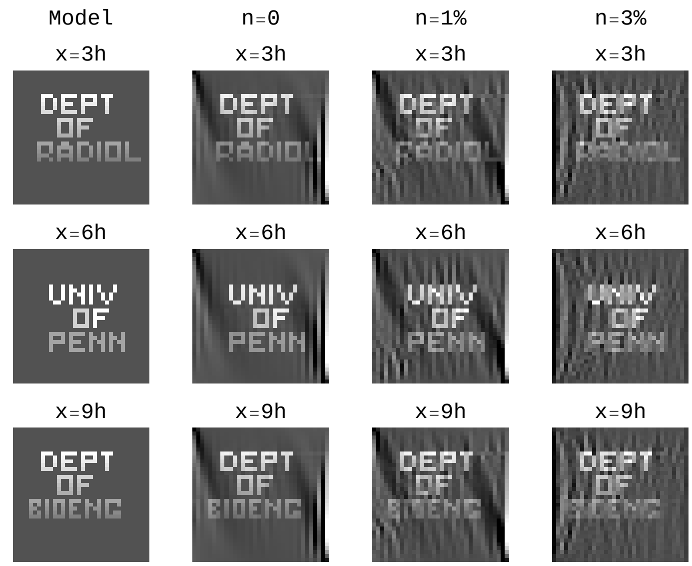

Model and reconstructed attenuation for various levels of noise n. Same color scale is used for all panels with the maximum (white) corresponding to $\mu_t = 0.28h^{-1}$ and the minimum (black) to $\mu_t = 0$. Only slices $x = 3h$, $x = 6h$ and $x = 9h$ are shown (the missing slices do not exhibit any visible "cross talk").

distance $\Delta x = h$. For each slice, the source positions were $x = x_{\rm slice}$, $y = nh$, $z = 0$, with n being integers. Seven consecutive slices were obtained, starting from the slice $x_{\rm slice} = 3h$. The reconstruction area inside each slice was $44h \leq y \leq 77h$, $4h \leq z \leq 37h$, with the field of view $34h \times 34h$. In the example shown in the Figure, the value of $\mu_s L_z$ (the number of scattering lengths in the sample thickness) was equal to 3.2.

The target was a set of absorbing inclusions formed in the shape of letters, with absorption varying from $0.06h^{-1}$ to $0.2h^{-1}$. The inclusions were concentrated only in three layers: $x = 3h$, $x = 6h$ and $x = 9h$, as shown in the columns marked "model". To model noise in the measured data, we first scaled and rounded off the specific intensity obtained from the RTE forward solver so that it was represented by a 16-bit integer, similar to measurements by digital CCD cameras. Then a statistically-independent positive-valued random variable was added to each measurement. The random variables were evenly distributed in the interval $[0, nI_{\rm av}]$, where n is the noise level indicated in the figureq and $I_{\rm av}$ is the average measured intensity (a 16-bit integer).

Images were obtained by the regularized SVD pseudoinverse of the discretized version of broken-ray integral transform. It can be seen that the spatial resolution of the reconstructed images depends on the noise level and contrast and can be as good as one discretization step, h. The reconstruction is stable in the presence of noise and quantitative. Overall, the reconstructions demonstrate the image quality and level of detail which is customary in x-ray tomography but can hardly be expected in optical tomography with multiply scattered light.

[1] S. R. Arridge, "Optical tomography in medical imaging," Inverse Problems **15,** R41–R93 (1999).

[2] D. A. Boas, D. H. Brooks, E. L. Miller, C. A. DiMarzio, M. Kilmer, R. J. Gaudette, and Q. Zhang, "Imaging the body with diffuse optical tomography," IEEE Signal Proc. Mag. **18,** 57–75 (2001).

[3] R. C. Erdmann and C. E. Siewert, "Green's function for the one-speed transport equation in spherical geometry," J. Math. Phys. **9,** 81–89 (1968).

[4] E. W. Larsen, "Solutions of the steady, one-speed neutron transport equation for small mean free paths," J. Math. Phys. **15,** 299–305 (1974).